Biointerface Research in Applied Chemistry
Open-Access Journal (ISSN: 2069-5837)

Article
Volume 13, Issue 1, 2023, 96
https://doi.org/10.33263/BRIAC131.096

Biocompatible Electroconductive Matrices for Tissue Engineering: A Comparative Study

Mikhail A. Shishov [1,2,*], Irina Yu. Sapurina [2], Natalia V. Smirnova [2], Vladimir E. Yudin [1,2]

[1] Institute of Macromolecular Compounds RAS,199004 Saint Petersburg, Russia
[2] Peter the Great Saint Petersburg Polytechnic University, 195251 Saint Petersburg, Russia
* Correspondence: shv_misha@mail.ru (M.A.S.);

Scopus Author ID 37071203600
Received: 11.12.2021; Accepted: 5.01.2022; Published: 12.02.2022

Abstract: Electroconductive polymer matrices intended for use in tissue engineering were prepared of various biocompatible polymers (polyimide, chitosan, copolyamide) modified with different conductive additives (graphene, carbon nanotubes, polypyrrole). Biocompatibility of matrices derived from composite materials was confirmed using human dermal fibroblast culture. Conducting properties of the matrices in the dry state and in physiological solution were investigated upon applying cyclic external potential. The influence of electron-conducting and ion-conducting components of the obtained composites on the current passing through the matrix and the shape of the current sweep is discussed.

Keywords: electroconductive extracellular matrix; tissue engineering; electronic and ionic conductivity.

1. Introduction

Among serious problems that hinder the transplantation of living tissues are immune rejection and lack of organs for implantation. New areas of medicine - cell transplantology, tissue engineering, and biomedical device technology - have been developed to meet these challenges. [1, 2]. Modern technologies involve the development of methods for the regeneration of native tissues of the patient; the ultimate purpose of this approach is to recover lost or damaged organs. These technologies are based on stimulating patient tissue regeneration to restore its structure and function [3-7]. One of the key elements of regenerative technologies is represented by extracellular matrices (ECM) designed for *in vitro* seeding with target cells. In addition, biocompatible materials are used as part of biomedical devices for noninvasive methods of diagnosis and treatment [6-8].

Many human cells (neurons, cardioblasts, fibroblasts, osteoblasts) are electrically active. It has been found that their growth can be stimulated by applying electrical signals to the matrix containing the cells [7, 8]. It has been demonstrated that electrostimulation influences fundamental aspects of vital cell activity and behavior (adhesion, migration, proliferation) and, besides, may control the differentiation of stem cells [9-11]. These extracellular matrices were used as scaffolds repairing peripheral nerves. The spinal cord injury treatment has been studied *in vivo* in guinea pigs, dogs, and humans in Phase I clinical trials and has proven effective. The studies have shown that electrostimulation increases neurite initiation, enhances axon growth rates, and affects the direction of neurite growth [12,13]. Conducting biomaterials have great potential in cardiac repair and regeneration. They can

improve cardiac functions: the electrical impulse propagation and synchronal heart contraction and thereby support the infarcted heart and correct arrhythmia [14,15].

Another direction is bone and skin tissue engineering and regeneration by using electrostimulation. The positive results of *in vitro* studies were duplicated of *in vivo* studies on the animal, then in clinical trials. Osteo- and skin-conduction and accelerated healing were observed [16,17]. The biocompatible conducting matrix can be used as the electrode material for *in vivo* electronics. Such matrices are flexible, stretchable, possess a large surface area, and integrate well with living tissues. They can be utilized as sensors for tissue monitoring, neural recording electrodes, electrostimulation, and drug delivery [18-20]. Therefore, it is important to develop electrically conducting extracellular matrices that will allow one to perform electrostimulation of cells and thus improve the efficiency of tissue therapy and accelerate regeneration.

As a rule, electroconductive extracellular matrices are composite materials. The main component of a matrix is a biocompatible polymer (dielectric or ionic conductor), whose mechanical properties (strength, elasticity) and surface characteristics (relief, free energy, charge) of which are almost similar to living tissue [21]. These are mainly natural polymers (chitosan, polylactides, gelatin, alginate, etc.) [22-28]. However, non-toxic synthetic polymers (siloxanes, polyimides, copolyamides, etc.) are also used; they are more stable than natural macromolecules and possess better mechanical properties [24, 29, 30]. To impart conductivity to a dielectric polymer, a biocompatible electrically conductive component is added (carbon materials or conducting polymers, noble metal particles (very rarely), [5, 6]. The most popular carbon materials are carbon nanotubes and graphenes with high conductivities and large specific surface areas [31-33]. The most frequently used conductive polymers are polyaniline and polypyrrole which demonstrate high conductivity and stability [5, 7, 9].

The electroconductive component should be strongly bound to the dielectric polymer and uniformly distributed within the polymer in order to provide a low percolation threshold and the maximum homogeneity of conducting and mechanical properties of the resulting composite matrix. In order to obtain a positive effect of electrostimulation, it is also necessary that the exposure of cells be adapted to the stability range of living tissues. Thus, highly conductive matrices can cause cell death due to exposure to currents exceeding their survival threshold. In contrast, insufficiently conductive (excessively resistive) matrices can lead to overheating due to applied voltage, which can cause cell death due to protein denaturation [34, 35]. Therefore, a wide variety of extracellular matrices are required for numerous applications.

In this paper, a comparative study of the conductive and capacitive characteristics of materials intended to manufacture electrically conductive matrices and devices for biomedical applications is carried out. The role of both different polymers and fillers that ensure the electrical conductivity of the composite material is considered. Biocompatibility of matrices based on the investigated material samples was shown in interaction with a culture of human dermal fibroblasts.

2. Materials and Methods

2.1. Electroconductive extracellular matrices.

CPA-PPy (the aliphatic copolyamide (CPA)/polypyrrole (PPy) composite containing 3–4 wt.% of PPy). The composite was prepared by casting CPA film (PA 6/66-3, "Anid OOO", Russia) from water/ethanol solution followed by surface modification of the film with

polypyrrole nanolayer in the course of the *in situ* oxidative polymerization of pyrrole (Fluka) [29].

CS-SWCNT (the chitosan (CS)/single-wall carbon nanotubes (SWCNT) composite containing 3 wt.% of SWCNT. The composite was obtained by mixing 4 wt.% aqueous solutions of chitosan CS (Biolog Heppe GmbH, Germany, MM = (1.64-2.1)×105, deacetylation degree DD = 92%) and an aqueous suspension of single-wall carbon nanotubes (SWCNT) (Carbon Chg, Russia) followed by film casting and drying [36].

PI-G (the polyamide (PI)/graphene (G) composite containing 3 wt.% of G). This product was obtained by polycondensation of poly(amido acid) (1,3-bis-(3,3'-4,4' – dicarboxyphenoxy)benzene) and diamine (4,4'-bis-(4-aminophenoxy)biphenyl) in N-methyl-2-pyrrolidone. The graphene suspension («GRAPHENE MATERIALS») was introduced together with the poly(amido acid). The composite films were prepared by thermal cyclization during stepwise heating from 100 to 300°C [37].

All composites were obtained in the form of homogeneous black films 50±10 μm thick. Before measurements, all films were repeatedly rinsed with distilled water and neutral physiological solution, then dried under normal conditions until the constant weight was reached.

The resistivity of films was determined by the four-point method using a Keithley 2010 voltmeter/ammeter and a Keithley 237 current source.

The water contact angles were determined using a DSA30 analyzer (Kruss, Germany). The measurements were performed at room temperature; distilled water was used.

Conductive and capacitive properties of ECM were studied with the use of the special cell made of inert and heat-resistant Teflon [36]. The electrodes (platinum wire 1 mm thick) were placed onto the studied sample and fixated the sample on the cell bottom. The electrode length was 25 mm, the distance between electrodes was 9 mm. The experiments involved ECM of the same size (35×9 mm) placed onto the cell bottom and fixated with electrodes. Before biocompatibility tests, the samples were sterilized in an autoclave (140°C, 40 min) together with the Teflon cell. The measurements were performed with the use of the Potentiostat/Galvanostat ELINS P-30J, which allowed for measuring currents ranging from 10 nA to 2 A and voltages from 80 μV to 15 V. The maximum rate of registration was 1580 points/sec.

2.2. Biocompatibility studies.

The human dermal fibroblasts obtained from conditionally healthy donors (Cell Culture Collection, Institute of Cytology RAS, Saint Petersburg) were used in the biological studies. The cells were cultivated in the complete nutrient medium (DMEM, Paneco, Russia) that additionally contained 1% of L-glutamine (200 mM), 10% of fetal bovine serum, 1% of antibiotics (penicillin 100 units/mL, streptomycin 100 μg/mL), and 1% of antimycotic agent (amphotericin B, 250 μg/mL) (all reagents: Gibco, USA). The cells were cultivated in a CO_2 incubator (Thermo Fisher Scientific, USA) at 37°C and high humidity; the CO_2 concentration was 5%. The cells of late passages (up to 15) were used. The amounts of viable cells contacting with ECM were determined by MTT tests that involved the use of the tetrazolium salt (3-(4,5-dimethylthiazol-2-yl)-2,5-diphenyltetrazolium bromide) (Thermo Fisher Scientific, USA) according to the standard technique [38]. The optical density of the formazan solution that correlated with the amount of viable cells was measured with a SPECTROstar Nano spectrophotometer at a wavelength of 570 nm. Table 1 presents the percentages of viable cells

contacting with extracellular matrices found in 4 days after the beginning of cultivation compared to those grown on the control samples. Methods of parametric statistics were used for statistical processing of the obtained data. The properties of the obtained composite films are also given in Table 1.

Table 1. Resistivity, hydrophobicity, and biocompatibility of the studied composite films.

Property \ Composite	CPA-PPy	CS-SWCNT	PI-G
Conductivity (S/cm) Four-point method	0.004±0.0005	0.02±0.005	5±0.05
Hydrophobicity Water contact angle	0	45±2	60±2
Biocompatibility MTT tests, (% of viable human dermal fibroblasts cells in comparison with the control experiment)	71±2	33±1	60±3

3. Results

A distinguishing feature of an electrical circuit, which includes a biological object, is that the external components of this circuit (the current source, instruments, metal wires) are electronic conductors, while a living tissue is an ionic conductor. When a potential is applied, an electric layer of oppositely charged ions (double electric layer) appears at the interface between ionic and electronic conductors; this layer compensates for the external potential and decreases the voltage in the circuit [39, 40]. It is known that alternating and impulse currents have a beneficial effect on cells [41, 42]. When the polarity of the external circuit is changed, the double electric layer rearranges itself; the existing ions are substituted for ions of the opposite signs. The time required for forming the double electric layer in an aqueous solution of an electrolyte depends on ion mobility and usually ranges of seconds [43]. Suppose the polarity of the electrode is maintained for long periods of time. In that case, the time dependence of current differs from the time dependence of potential due to the contribution of the change in the double electric layer [44].

When performing electrical stimulation of cells and tissues, it is important to understand which real currents flow through ECM and how they influence a biological object. The present work studied the electrical properties of three matrices prepared from different polymers and containing different conductive components. The preliminary experiments demonstrated that the studied matrices were non-toxic and compatible with human fibroblasts (Table 1). Electrical studies involved both dry matrices (investigated at ambient temperature and humidity) and the films immersed into an aqueous solution of an electrolyte (saline, 0.9% wt. NaCl); i.e., in physiological conditions similar to those of electrostimulation were created. Fig. 1 presents the voltage-current relationships obtained for dry and wet CPA-PPy, CS-SWCNT, and PI-G films. The U-shaped signal (±100 mV) with polarity changed every 30 s (0.03 Hz) was applied to the matrices placed into the electrostimulation cell and fixated with parallel electrodes. The choice of external circuit parameters depended on the restrictions imposed on the experiments with biological objects. On the one hand, the value of electrode potential is close to membrane resting potentials (–70 mV) and action potentials (+40 mV) of living cells [41]; at the same time, it lies far from the boundaries of the "stability window" of the electrolyte solution (1.23 V), because approaching its boundaries may cause the formation of free radicals toxic for living organisms [35]. The frequency of potential change (0.03 Hz) was lower than

the rates of rearrangements of the double electric layer, which made it possible to monitor its formation and its influence on the currents flowing through ECM.

In the dry state (when ionic conductivity is suppressed, and only the electron-conducting component of ECM manifests itself), the CPA-PPy sample has the lowest specific conductivity; specific conductivity of CS-SWCNT is several times higher, and for the PI-G sample, this parameter is even higher (by several orders of magnitude, see Table 1). This is also confirmed by the slopes of voltage-current relationships of dry ECM measured in the cell (Figure 1). The voltage-current relationships for all matrices indicate ohmic behavior within the studied range of potentials, and no current saturation with increasing potential is observed.

The introduction of the physiological solution into the measurement cell leads to dramatic changes in voltage-current relationships for the CPA-PPy and CS-SWCNT matrices. The conductivity of the CPA-PPy sample increases by 10 times, while the conductivity of the CS-SWCNT film, on the contrary, decreases by 4 times. The voltage-current relationships for wet matrices are curves reaching a plateau. Meanwhile, the shape of the voltage-current relationship of PI-G does not change upon introducing electrolyte; the consistent ohmic dependence with the same slope (i.e., the same current) is observed.

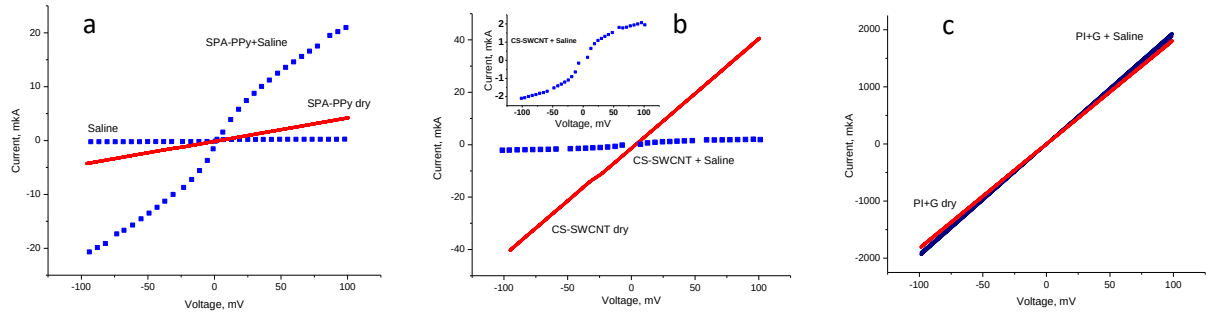

Figure 1. Voltage-current relationships: (**a**) CPA-PPy; (**b**) CS-SWCNT; (**c**) PI-G in the dry state (red) and in physiological solution (blue). Fig. 1 (**a**) shows the voltage-current relationship for electrodes of measurement cell in saline. Inset in Fig. 1 (**b**) shows the non-linear voltage-current relationship for CS-SWCNT in saline in the low current range.

Figure 2 shows the physiological solution's cyclic voltammograms obtained for the CPA-PPy, CS-SWCNT, and PI-G samples. The area enclosed by the curve is proportional to the electrochemical capacity, i.e., its ability to accumulate electric charges. For materials that do not possess redox activity, electrochemical capacity is related to the contribution of the double electric layer formed at the phase interface [45, 46]. It is seen that the electrochemical capacity of the CPA-PPy sample is higher than that of CS-SWCNT, while the PI-G sample does not have any electrochemical capacity.

Figure 3 shows the sweeps of real currents flowing through ECM in the dry state and saline when the potentials (±100 mV) with polarity changed every 30 s was applied to ECM by the external source (Figure 3a). First, it should be noted that continuous potential cycling for several hours does not cause any decrease in the current flowing through dry and wet samples [36]. Electrochemical characteristics of the matrices are also reproducible after prolonged storage under normal conditions in dry and saline states. This indicates the stability of the studied materials and the possibility of their long-term storage and repeated usage, which is important in cell therapy.

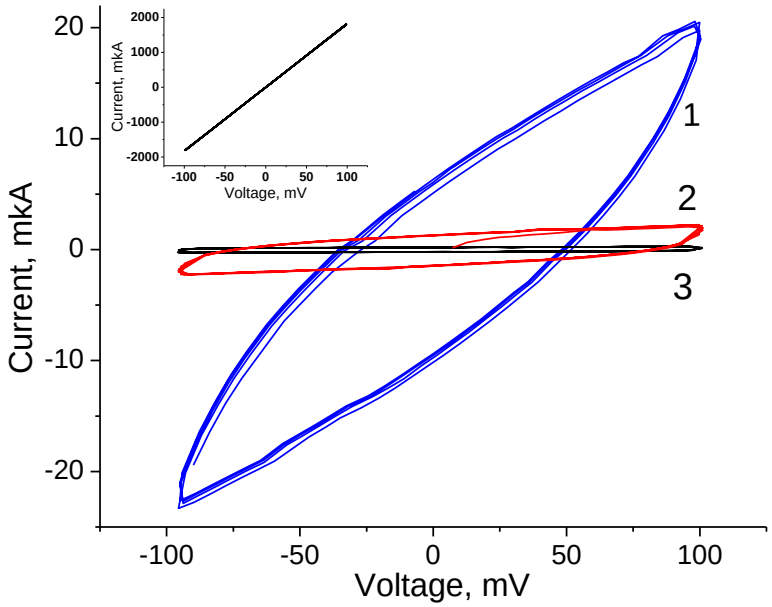

Figure 2. Cyclic voltammograms: 1 – CPA-PPy, 2 – CS-SWCNT, 3 – electrodes of measurement cell in saline. Inset: cyclic voltage-current relationship for PI-G in saline. Scanning rate: 6.6 mV/s.

It can be seen that for all ECM, the current immediately changes direction in the point of electrode polarity change. In the case of the PI-G matrix (Figure 3c), currents change together with changes in potential and demonstrate the rectangular current sweep, independently of its state (dry or wet). When CPA-PPy and CS-SWCNT were studied in the dry state, currents immediately changed together with the external potential and gave the rectangular current sweeps (Figure 3a,b).

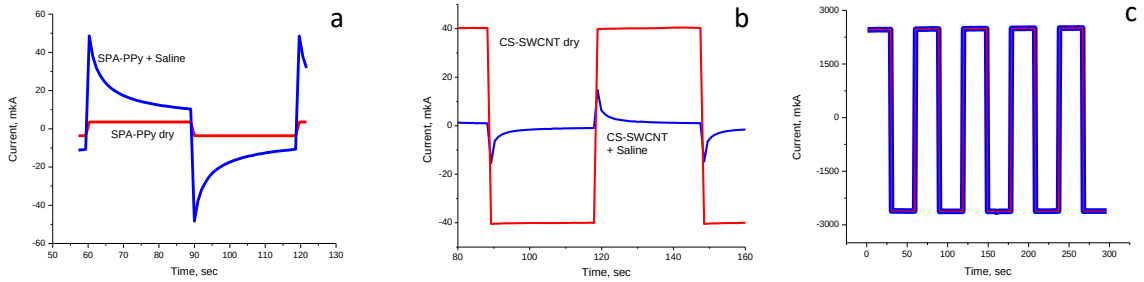

Figure 3. Real currents flowing through ECM: (**a**) CPA-PPy; (**b**) CS-SWCNT; (**c**) PI-G in the dry state (red) and in physiological solution (blue) upon application of external U-shaped potential ±100 mV, whose polarity was changed every 30 s.

However, a more complex current sweep is observed in saline. After polarity change, the current through CPA-PPy and CS-SWCNT matrices rises immediately, then decreases exponentially. It is indicative that for CPA-PPy, the initial peak current in the electrolyte (50 µA) is considerably higher than that in the dry state (5 µA), while for CS-SWCNT, the reverse is true (the initial current in saline (10 µA) is lower than that in the dry state (40 µA). Within the next 30 s, the current in CPA-PPy decreases to 5 µA, and in CS-SWCNT, the current decreases to 1–2 µA.

4. Discussion

The presented results show that under the conditions used in electrostimulation, various ECM may generate current sweeps differing in shape and magnitude; the currents do not necessarily coincide with current parameters for dry matrices. This is explained by the fact that

composite matrices include conductors with different conductivity types (electronic and/or ionic). In the dry state, ionic conductivity is virtually suppressed. The samples demonstrate only an electronic component of current, which responds immediately to any changes in potential and changes accordingly with a potential sweep. In physiological solution, ionogenic groups in ion-conductive ECM become hydrated and produce ions. Therefore, in addition to the electronic current, there is the contribution of the ionic current, which is characterized by inertia due to the low mobility of charge carriers. Hydration efficiency largely depends on the hydrophilicity of a matrix (Table 1). Let us consider the influence of physiological solution on contributions made by electronic and ionic currents for each studied ECM.

The PI-G composite contains only the electronic conductor (graphene). Polyimide is a dielectric material; it does not contain any ionogenic groups and does not make an ionic contribution to total conductivity (Figure 4) [47]. Therefore, both in dry and in wet matrices, only electronic currents appear and completely reproduce the voltage sweeps. The PI-G composite has low hydrophilicity and thus is poorly wetted with the electrolyte solution. Because of this, the double electric layer involving the saline ions (Na^+Cl^-) is not formed completely on the PI-G interface, and this ECM practically does not possess electrochemical capacity (Figure 2).

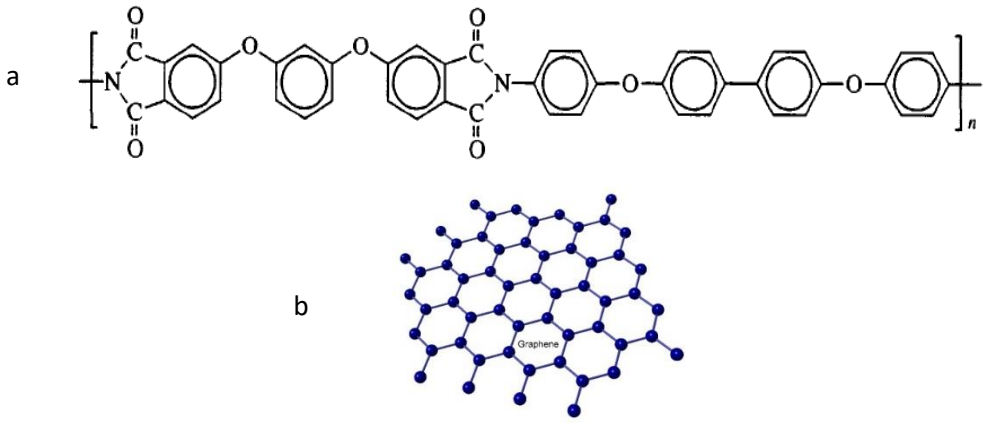

Figure 4. Structural formulas of the monomeric unit of (**a**) polyimide (dielectric) and (**b**) graphene (electronic conductor).

The CS-SWCNT matrix consists of chitosan that contains ionogenic amino group $–NH_3^+$ and acts as an ionic conductor [48]. The second component (carbon nanotubes) is an electronic conductor (Figure 5.). Thus, CS-SWCNT is a two-component material containing substances with different conductivity types.

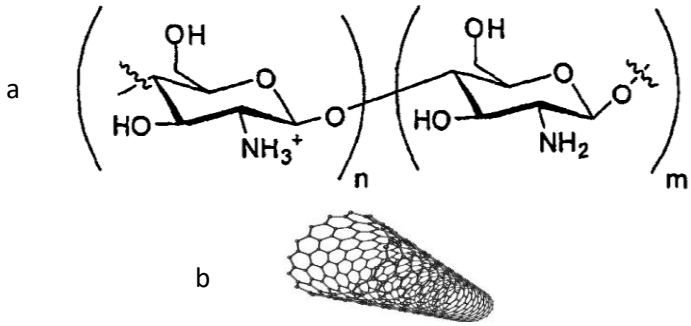

Figure 5. Structural formulas of (**a**) the ionic conductor CS and (**b**) electronic conductor SWCNT. Indices n and m show amounts of monomer units of CS with ionogenic protonated groups ($–NH_3^+$) and non-ionogenic $–NH_2$ groups, respectively.

Chitosan is more hydrophilic than PI and thus is well wetted by water; the resulting –NH_3+ ions and Na+Cl- ions intercalated by the matrix create the double electric layer at the CS-SWCNT interface [40]. Since SWCNT are well dispersed and creates a percolation network in CS, the area of the double electric layer is large. Therefore, the effect of compensation of the external potential and a decrease in the current will also be noticeable [49]. During changing potential in saline, the matrix generates currents ranging from 10 to 1-2 μA, which is lower than the current appearing in the dry matrix (40 μA). Measurements of electrochemical capacity (Figure 2) confirm that the capacity of the double electric layer in the CS-SWCNT film is higher than that of electrodes in the electrolyte (Figure 2). Thus, the interface area between the electronic conductor (percolation network of SWCNT) and an ionic conductor (CS) is large and can provide a considerable compensating effect.

The CPA-PPy matrix consists of a dielectric without ionogenic groups (CPA) and a conducting polymer PPy, Figure 6). Polypyrrole demonstrates both ionic and electronic conductivities. Electron transport in PPy is realized by delocalized cation-radical centers, the so-called positive polarons, which move along the conjugation system formed by polymer chains and their aggregates [50, 51]. Ion transport is performed by counterions that compensate polaron charge [52]. Thus, the same structures generate both electronic and ionic currents.

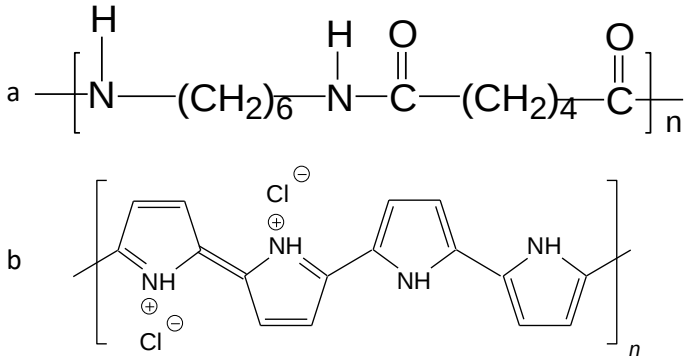

Figure 6. Structural formulas of the monomer unit of (**a**) the CPA dielectric and the mixed electron and (**b**) ion-conductor PPy. Symbol (+) denotes carriers of electron current (positive polaron).

It is known that PPy conductivity increases naturally with increasing humidity [53]. For this reason, PPy has proved to be efficient as a detecting element of humidity sensors that work on the principle of chemoresistor [54, 55]. Additional hydration of polarons leads to an increase in the mobility of charge carriers of both types. The highest conductivity values are observed in electrolyte solutions [53]. The peak current value registered in the CPA-PPy matrix immersed in saline is equal to 50 μA, which is 10 times higher than the current in the dry matrix. Then, the total current decreases slowly down to 10 μA, which is 2 times higher than the currents in the dry material.

The electrochemical capacity of the CPA-PPy matrix is considerably higher than that of the CS-SWCNT and PI-G samples (Figure 2). On the one hand, this can be explained by the extremely high hydrophilicity of PPy that includes electrolyte ions in its structure (Table 1). Besides, the capacity of PPy is additionally enhanced by the redox properties of the polymer, i.e., its ability to reversibly change the amount of charged groups after changing external potential [52]. Capacitive characteristics of ECM also play an important role during the electrostimulation of cells. High local concentration of potentials caused by inhomogeneous composition and structure of ECM may cause the generation of free radicals that are toxic for living cells. The excess potential may appear at the butt of a nanotube or on the facet of a graphene sheet protruding above the matrix surface. The high capacity of the matrix smooths

out the voltage jumps and thus eliminates this problem, which makes it possible to use comparatively high external potentials in electrostimulation.

5. Conclusions

Conductive properties of three different biocompatible extracellular matrices (ECM) based on various polymers modified with electron-conducting and electron/ion-conducting components were compared. The measurements involved the dry matrices (the ionic conductivity is suppressed) and the matrices immersed in physiological solution. The application of cyclic potential (±100 mV) with polarity changing every 30 s (0.03 Hz) to ECM allowed us to observe the double electric layer's formation and study the contributions of the ionic carrier into the total current.

It was demonstrated that in the case of the ECM with low hydrophilicity containing only electron charge carriers (PI-G), the currents flowing through the matrix in the dry and wet states are similar and change together with potential. If the matrix possesses both electronic and ionic conductivities, it is necessary to understand where the carriers of electronic and ionic currents are localized. When mixed conductors (conducting polymers polyaniline and polypyrrole) are used, both conductivity types are enhanced in physiological solution; therefore, the conductivity of the wet CPA-PPy matrix is higher than that of the dry sample. On the contrary, the combination of substances with different types of conductivity (CS-SWCNT) may lead to the compensation of electronic current by the ionic conductor and a decrease in the current in physiological solution compared to that in the dry ECM.

Funding

This work was funded by the Russian Science Foundation, project no. 19-73-30003.

Acknowledgments

The authors thank Dr. Vera Kodolova-Chukhontseva and Dr. Almaz Kamalov for samples used for experiments.

Conflicts of Interest

The authors declare that they have no conflict of interest.

References

1. Kir, D.; Patel, M.J.; Munagala, M.R. What Is the Status of Regenerative Therapy in Heart Failure? *Current Cardiology Reports* **2021**, *23*, 146-155, https://doi.org/10.1007/s11886-021-01575-3.
2. Hashimoto, H.; Olson, E.N.; Bassel-Duby, R. Therapeutic approaches for cardiac regeneration and repair. *Nat Rev Cardiol*. **2018**, *15*, 585–600, https://doi.org/10.1038/s41569-018-0036-6.
3. Shanley, L.C.; Mahon, O.R.; Kelly, D.J.; Dunne, A. Harnessing the innate and adaptive immune system for tissue repair and regeneration: Considering more than macrophages. *Acta Biomaterialia* **2021**, *133*, 208-221, https://doi.org/10.1016/j.actbio.2021.02.023.
4. Elalouf, A. Immune response against the biomaterials used in 3D bioprinting of organs. *Transplant Immunology* **2021**, *69*, 101446, https://doi.org/10.1016/j.trim.2021.101446.
5. Bendrea, A-D.; Cianga, L.; Cianga, I. Review Paper: Progress in the Field of Conducting Polymers for Tissue Engineering Applications. *Journal of Biomaterials Applications* **2011**, *26*, 1-83, https://doi.org/10.1177/0885328211402704.

6. Nekounam, H.; Shayan, G.; Allahyari, Z.; Samadian, H.; Nazeri, N.; Shokrgozar, M., A.; Faridi-Majidi R. Electroconductive scaffolds for tissue regeneration. Current opportunities, pitfalls, and potential solutions. *Materials Research Bulletin* **2021**, *134*, 111083, https://doi.org/10.1016/j.materresbull.2020.111083.
7. Huang, Z.B.; Yin. G.F.; Liao, X.M.; Gu, J.W. Conducting polypyrrole in tissue engineering applications. *Front. Mater. Sci.* **2014**, *8*, 39–45, https://doi.org/10.1007/s11706-014-0238-8.
8. Guixin, S.; Rouabhia, M.; Meng, S.; Zhang, Z. Electrical stimulation enhances viability of human cutaneous fibroblasts on conductive biodegradable substrates. *Journal of Biomedical Materials Research Part A* **2007**, *84A*, 1026-1037, https://doi.org/10.1002/jbm.a.31337.
9. Rowlands, A.S.; Cooper-White, J.J. Directing phenotype of vascular smooth muscle cells using electrically stimulated conducting polymer. *Biomaterials* **2008**, *29*, 4510–4520. https://doi.org/10.1016/j.biomaterials.2008.07.052.
10. Balint, R.; Cassidy, N.J.; Cartmell, S.H. Electrical Stimulation: A Novel Tool for Tissue Engineering. *T*issue *Engineering Part B* **2013**, *19*, 48-57, https://doi.org/10.1089/ten.teb.2012.0183.
11. Ramirez-Fernandez, O.; Zuniga-Aguilar, E.; A review from mesenchymal stem-cells and their small extracellular vesicles in tissue engineering. *Biocell* **2022**, *46*, 325-338, https://doi.org/10.32604/biocell.2022.016892.
12. Zhao, Y.; Liang, Y.; Ding, S.; Zhang, K.; Mao, H.-G.; Yang, Y. Application of conductive PPy/SF composite scaffold and electrical stimulation for neural tissue engineering. *Biomaterials* **2020,** *255*, 120164, https://doi.org/10.1016/j.biomaterials.2020.120164.
13. Shapiro, S.; Borgens, R.; Pascuzzi, R.; Roos, K.; Groff, M.; Purvines, S.; Ben, R.; Hagy, S.; Nelson, P. Oscillating field stimulation for complete spinal cord injury in humans: a phase 1 trial. *J Neurosurg Spine* **2005**, *2*, 3-10, https://doi.org/10.3171/spi.2005.2.1.0003.
14. Cui, Z.; Yang, B.; Li. R.-K. Application of Biomaterials in Cardiac Repair and Regeneration *Engineering* **2016**, *2*, 141–148, http://dx.doi.org/10.1016/J.ENG.2016.01.028.
15. Zhang, C.; Hsieh, M.-H.; Wu, S.-Y.; Li, S.-H.; Wu, J.; Liu, S.-M.; Wei, H.-J.; Weisel, R.D.; Sung, H.-W.; Li, R.-K.A. Self-doping conductive polymer hydrogel that can restore electrical impulse propagation at myocardial infarct to prevent cardiac arrhythmia and preserve ventricular function. *Biomaterials* **2020,** *231*, 119672, https://doi.org/10.1016/j.biomaterials.2019.119672.
16. Shi, G.; Zhang, Z.; Rouabhia. M. The regulation of cell functions electrically using biodegradable polypyrrole–polylactide conductors. *Biomaterials* **2008**, *29*, 3792–3798, https://doi.org/10.1016/j.biomaterials.2008.06.010.
17. Liang, Y.; Zhao, X.; Hu, T.; Chen, B.; Yin, Z.; Ma, P.X.; Guo, B. Adhesive hemostatic conducting injectable composite hydrogels with sustained drug release and photothermal antibacterial activity to promote full-thickness skin regeneration during wound healing. *Small* **2019**, *15*, 1900046, https://doi.org/10.1002/smll.201900046.
18. Heo, D.N.; Kim, H.J.; Lee Y.J.; Heo, M.; Lee, S.J.; Lee, D.; Do, S.H.; Lee, S.H.; Kwon, I.K. Flexible and highly biocompatible nanofiber-based electrodes for neural surface interfacing. *ACS Nano* **2017**, *11*, 2961–2971, https://doi.org/10.1021/acsnano.6b08390.
19. Park, J.; Choi, S.; Janardhan A.H.; Lee, S.Y.; Raut, S.; Soares, J.; Shin, K.; Yang, S.; Lee, C.; Kang, K.W.; Cho, H.R.; Kim, S.J.; Seo, P.; Hyun, W.; Jung, S.; Lee, H.J.; Lee, N.; Choi, S.H.; Sacks, M.; Lu, N.; Josephson, M.E.; Hyeon, T.; Kim, D.H.; Hwang, H.J. Electromechanical cardioplasty using a wrapped elasto-conductive epicardial mesh. *Science Translational Medicine* **2016**, *8*, 344, https://doi.org/10.1126/scitranslmed.aad8568.
20. Wang, L.; Wu, Y.; Hu, T.; Guo, B.; Ma, P.X. Electrospun conductive nanofibrous scaffolds for engineering cardiac tissue and 3D bioactuators. *Acta Biomater* **2017**, *59*, 68–81, https://doi.org/10.1016/j.actbio.2017.06.036.
21. Viola, M.; Piluso, S.; Groll, J.; Vermonden, T.; Malda, J.; Castilho, M. The Importance of Interfaces in Multi-Material Biofabricated Tissue Structures. *Advanced Healthcare Materials* **2021**, *10*, 2101021, https://doi.org/10.1002/adhm.202101021.
22. Chahal, S.; Kumar, A.; Hussian, F.S.J. Development of biomimetic electrospun polymeric biomaterials for bone tissue engineering. A review. *Journal of Biomaterials Science-Polymer Edition* **2019**, *30*, 1308-1355, https://doi.org/10.1080/09205063.2019.1630699.
23. Amin, M.R.; Mahmud, M.A.; Anannya, F.R. Natural Fiber Reinforced Starch Based Biocomposites. *Polymer Science Series A* **2019**, *61*, 533-543, https://doi.org/10.1134/S0965545X1905016X.

24. Jangid, N.K.; Hada, D.; Rathore, K. Chitosan as an emerging object for biological and biomedical applications. *Journal of Polymer Engineering* **2019**, *39*, 689-703, https://doi.org/10.1515/polyeng-2019-0041.
25. Zhu, T.; Mao, J.; Cheng, Y.; Liu, H.; Lv, L.; Ge, M.; Li, S.; Huang, J.; Chen, Z.; Li, H.; Yang, L.; Lai, Y. Recent Progress of Polysaccharide-Based Hydrogel Interfaces for Wound Healing and Tissue Engineering. *Advanced Materials Interfaces* **2019**, 1900761,1-22, https://doi.org/10.1002/admi.201900761.
26. Rezaei, F.S.; Sharifianjazi, F.; Esmaeilkhanian, A.; Salehi, E. Chitosan films and scaffolds for regenerative medicine applications. A review. *Carbohydrate Polymers* **2021**, *273*, 118631 https://doi.org/10.1016/j.carbpol.2021.118631.
27. Mahendiran, B.; Muthusamy, S.; Selvakumar, R.; Rajeswaran, N.; Sampath, S.; Jaisankar, S.N.; Krishnakumar, G.S. Decellularized natural 3D cellulose scaffold derived from Borassus flabellifer (Linn.) as extracellular matrix for tissue engineering applications. *Carbohydrate Polymers* **2021**, *272*, 118494 https://doi.org/10.1016/j.carbpol.2021.118494.
28. Kirillova, A.; Yeazel, T.R.; Asheghali, D.; Petersen, S.R.; Dort, S.; Gall, K.; Becker, M.L. Fabrication of Biomedical Scaffolds Using Biodegradable Polymers. *Chemical Reviews* **2021**, *121*, 11238-11304, https://doi.org/10.1021/acs.chemrev.0c01200.
29. Smirnova, N.V.; Sapurina, I.Y.; Shishov, M.A.; Kolbe, K.A.; Ivan'kova, E.M.; Matrenichev, V.V.; Yudin, V.E. Composite Matrices Based on Copolyamide and Polypyrrole for Tissue Engineering. *Technical Physics* **2020**, *65*, 1574-1579, https://doi.org/10.1134/S1063784220100217.
30. Sapurina, I.Y.; Matrenichev, V.V.; Vlasova, E.N.; Shishov, M.A.; Ivan'kova, E.M.; Dobrovolskaya, I.P.; Yudin, V.E. Synthesis and Properties of a Conducting Material Based on Hybrid Nanofibers of Aliphatic Copolyamide and Polypyrrole. *Polymer Science Series B* **2020**, *62*, 116-124, https://doi.org/10.1134/S156009042001008X.
31. Oprych, K.M.; Whitby, R.L.D.; Mikhalovsky, S.V.; Tomlins, P.; Adu, J. Repairing Peripheral Nerves: Is there a Role for Carbon Nanotubes. *Adv. Healthcare Mater.* **2016**, *5*, 1253–1271, https://doi.org/10.1002/adhm.201500864.
32. Cervantes, S.A.; Jose, A.P.; Martínez, G.; Bernabeu-Esclapez, A.; Otero, T.F.; Meseguer-Olmo, L.; Paredes, J.I.; Cenis, J.L. Electrospun silk fibroin scaffolds coated with reduced graphene promote neurite outgrowth of PC-12 cells under electrical stimulation. *Materials Science and Engineering* **2017**, *79*, 315-325, https://doi.org/10.1016/j.msec.2017.05.055.
33. Jodati, H.; Yilmaz, B.; Evis, Z. *In vitro* and *in vivo* properties of graphene-incorporated scaffolds for bone defect repair. *Ceramics International* **2021**, *47*, 29535-29549, https://doi.org/10.1016/j.ceramint.2021.07.136.
34. Islam, M.; Lantada, A.D.; Mager, D.; Korvink, J.G. Carbon-Based Materials for Articular Tissue Engineering: From Innovative Scaffolding Materials Toward Engineered Living Carbon. *Advanced Healthcare Materials* **2021**, *11*, 2101834, https://doi.org/10.1002/adhm.202101834.
35. Sikorski, P. Electroconductive scaffolds for tissue engineering. Applications. *The Royal Society of Chemistry, Biomaterials Science* **2020**, *8*, 5583-5588, https://doi.org/10.1039/d0bm01176b.
36. Sun, Y–S. Electrical Stimulation for Wound-Healing: Simulation on the Effect of Electrode Configurations. *BioMed Research International* **2017**, *2017*, 5289041, https://doi.org/10.1155/2017/5289041.
37. Kolbe, K.; Shishov M.A.; Sapurina I.Yu.; Smirnova N.V.; Kodolova-Chukhontseva V.V.; Dresvyanina E.N.; Kamalov A.M.; Yudin V.E. Electrostimulation of human dermal fibroblasts on an electrically conductive matrix. *Technical Physics* **2021**, *91*, 2061-2068.
38. Smirnova, V. E.; Saprykina, N. N.; Lavrent'ev, V. K.; Popova, E. N. ; Kolbe, K.; Kuznetsov, D. A. ; Yudin, V. E. Mechanical Properties and Supramolecular Structure of Oriented Polyimide Films Filled with Carbon Nanofibers. *Polymer Science Series A* **2021**, *63*, 307-317, https://doi.org/10.1134/S0965545X21030123.
39. Kumar, P.; Nagarajan, A.; Uchil, P.D. Analysis of Cell Viability by the MTT Assay. *Cold Spring Harbor Protocols* **2018**, *6*, https://doi.org/10.1101/pdb.prot095505.
40. Allagui, A.; Benaoum, H.; Olendski, O. On the Gouy-Chapman-Stern model of the electrical double-layer structure with a generalized Boltzmann factor. *Physica A-Statistical Mechanics and its Applications* **2021**, *582*, 126252, https://doi.org/10.1016/j.physa.2021.126252.
41. Uematsu, Y. Electrification of water interface. *Journal of Physics-Condensed Matter.* **2021**, *33*, 423001, https://doi.org/10.1088/1361-648X/ac15d5.

42. Kumar, A.; Nune, K.C.; Misra, R.D.K. Understanding the response of pulsed electric field on osteoblast functions in three-dimensional mesh structures. *Journal of Biomaterials Applications* **2016**, *31*, 594-605, https://doi.org/10.1177/0885328216658376.
43. Pethig, R. Dielectrophoresis: Using inhomogeneous AC electrical fields to separate and manipulate cells. *Critical Reviews in Biotechnology* **1996**, *16*, 331-348, https://doi.org/10.3109/07388559609147425.
44. Sikiru, S. Ionic transport and influence of electromagnetic field interaction within electric double layer in reservoir sandstone. *Journal of Molecular Liquids* **2021**, *344*, 117675, https://doi.org/10.1016/j.molliq.2021.117675.
45. Jiang, Y.; Huang, J.B.; Mao, B.G.; An, T.Y.; , J.; Cao, M.H. Inside solid-liquid interfaces: Understanding the influence of the electrical double layer on alkaline hydrogen evolution reaction. *Applied Catalysis B-environmental* **2021**, *293*, 120220, https://doi.org/10.1016/j.apcatb.2021.120220.
46. Lamperski, S. Structural and thermodynamic properties of the electrical double layer in slit nanopores: A Monte Carlo study. *Journal of Chemical Physics* **2020**, *153*, 134703, https://doi.org/10.1063/5.0020905.
47. Derjaguin, B.V.; Krotova, N.A.; Karassev, V.V.; Kirillova, Y.M.; Aleinikova, I.N. Electrical phenomena accompanying the formation of new surfaces, and their role in adhesion and cohesion. *Progress in Surface Science* **1994**, *45*, 95-104, https://doi.org/10.1016/0079-6816(94)90039-6.
48. Yoonessi, M.; James, R. G.; Muhammad, S.; Daulton, T.L.; Kaner, R.B.; Meador, M.F. Fabrication of Graphene−Polyimide Nanocomposites with Superior Electrical Conductivity. *ACS Appl. Mater. Interfaces* **2017**, *9*, 43230−43238, https://doi.org/10.1021/acsami.7b12104.
49. He, X-M.; Liang, X-C.; Chen, X.; Yuan, B-F.; Zhou, P.; Zhang, L-N.; Feng, Y.-Q. High Strength and Hydrophilic Chitosan Microspheres for the Selective Enrichment of N-Glycopeptides. *Anal. Chem.* **2017**, *89*, 9712–9721, https://doi.org/10.1021/acs.analchem.7b01283.
50. Scarratt, L.R.J.; Trefalt, G.; Borkovec, M. Forces between interfaces in concentrated nanoparticle suspensions and polyelectrolyte solutions. *Current Opinion in Colloid & Interface Science* **2021**, *55*, 101482, https://doi.org/10.1016/j.cocis.2021.101482.
51. Singh, R.; Tandon, R.P.; Chandra, S. Evidence of small-polaron formation in polypyrrole. *Journal of Physics-Condensed Matter* **1993**, *5*, 1313-1318, https://doi.org/10.1088/0953-8984/5/9/015.
52. Huang, M.R.; Gu, G.L.; Ding, Y.B.; Fu, X.T.; Li, R.G. Advanced Solid-Contact Ion Selective Electrode Based on Electrically Conducting Polymers. *Chinese Journal of Analytical Chemistry* **2012,** *40*, 1454-1460, https://doi.org/10.1016/S1872-2040(11)60572-0.
53. Huang, H.; Karlsson, C.; Mamedov, F.; Stromme, M.; Gogoll, A.; Sjodin, M. Polaron Disproportionation Charge Transport in a Conducting Redox Polymer. *Journal of Physical Chemistry* **2017**, *121*, 13078-13083, https://doi.org/10.1021/acs.jpcc.7b03671.
54. Lippe, J.; Holze, R. In-situ spectroelectrochemical investigation of the solvent effect on polyaniline and polypyrrole. *Molecular Crystals and Liquid Crystals* **1991**, *208*, 99-108, https://doi.org/10.1080/00268949108233947.
55. De Aguiar, M.F.; Leal, A.N.R.; De Melo, C.P.; Alves, K.G.B. Polypyrrole-coated electrospun polystyrene films as humidity sensors. *Talanta* **2021**, *234*, 122636, https://doi.org/10.1016/j.talanta.2021.122636.